HIGH PERFORMANCE POSITION TRACKING WITH FRICTION COMPENSATION FOR AN ELECTRO-PNEUMATICAL ACTUATOR

Alina Voda, Laleh Ravanbod-Shirazi

Laboratoire d'Automatique de Grenoble
ENSIEG, B.P. 46, 38402 Saint Martin d'Hères, FRANCE
Alina.Voda@inpg.fr

Abstract: *In this paper, considering an asymmetrical Karnopp model of friction, a compensator is proposed to improve position tracking in an electro-pneumatic system. For such systems, model-based friction compensation is difficult due to the presence of actuator dynamics. The proposed compensator requires the presence of two control loops (force and position loop).*
For high velocity values, the compensator deals with Coulomb friction. For small velocity values, stick friction is cancelled, while for near-zero velocities, the position error is also considered in the compensator structure.
Not only the compensator but also the position controller has to be optimized for high performance tracking position, and periodic reidentiffication is necessary to overcome possible changes in the system . By simulation and real-time experiments it is shown that the position tracking error is minimized.

Keywords*: Karnopp model, friction compensation, electro-pneumatic actuator, PID control*

NOTATION

$y,\ \dot{y},\ \ddot{y}$	position, velocity, acceleration
r	position reference
F_e	applied force
$n_y,\ n_{Fe}$	position and applied force measurement noises
u	control signal
Pp, Pn	pressures in the right and left chambers of the cylinder
x_m	measurements of signal x
x_f	filtered signal x_m
$\dot{y}_f\ ,\ \ddot{y}_f$	velocity and acceleration found using filtered measured position
F_{ec}	computed applied force
F_f	friction force (torque)
F_{slip}	slip friction
F_{stick}	stick friction
$F_{\text{zero velocity}}$	friction force at zero velocity
F_{comp}	compensation force (torque)
m	mass of moving part
$F_{Cp,n}\ ,\ F_{Vp,n}$	Coulomb friction and viscous friction coeffcient for positive and negative velocities
$F_{Sp;n}$	saturation values of stick friction for positive and negative applied force
$d_{Vp;n}$	limited velocity during stick-positive slip and stick-negative slip
$\widehat{p}$	estimation of parameter p
P_{asym}	vector of asymmetrical Karnopp model parameters
h	sampling period
k_a	parameter of linear model of motor actuator
$k_1,\ k_2$	parameters of linear model of electro-pneumatic actuator
g_x	sensor gain of signal x
$S_p,\ S_n$	area of right and left chambers of cylinder
$C,\ C_F$	position and applied force controllers

k_i , T_i	PI controller parameters
k_d ,T_d,, €	PD controller parameters
N_c	variable determining zero velocity or stick friction compensation
N_d	time horizon used in the numerical derivation function
e_y , e_T	position error and its threshold value
$\hat{d}v_{p1}, \hat{d}v_{n1}$	maximum and minimum authorized velocities in the zero velocity boundary

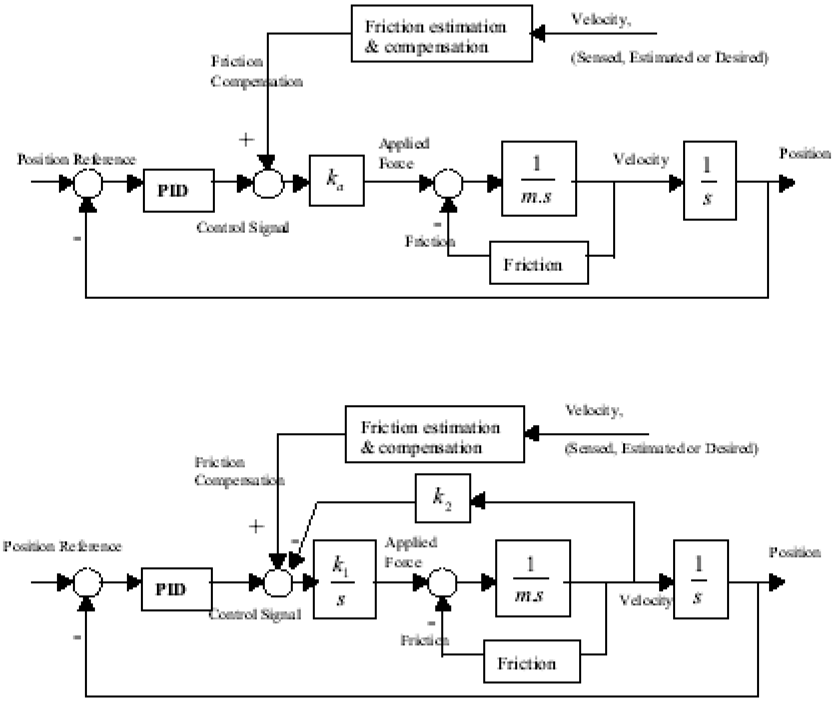

Figure 1: PID controller and model-based friction compensation in a dc-motor-driven system (up) and in an electro-pneumatic actuation system (down).

INTRODUCTION

Friction is a nonlinearity that is present in all machines with moving parts. It has received much attention due to its many indesirable effects such as oscillations, steady state error and power dissipation. In [1], a detailed discussion on friction phenomena and its compensation methods in different mechanisms is presented and many references are cited. As a rule, the compensation approaches are classified in model- based and non-model-based approaches.

- Non-model-based approach: In this approach, no friction model is used. Compensation is achieved by:

  1. Changing the position controller parameters: To overcome the steady state error produced by friction when a PD controller is used, the PD gains are increased, which is equivalent to increasing system stiffness. Thus, the high gain PD 4 control is the most successful in systems designed for high rigidity. In addition to the steady-state error, friction can produce limit cycles. This is the case when integral action is used, as in a PI(D) controller. To overcome this limit cycle, a dead-band block is used [15], the integral term is reset or adjusted [18, 4]. However, when such modifications are used, the steady state error and the limit cycle may not be completely eliminated [1].

  2. Applying dither: The best known non-model-based method used for friction compensation in systems with non negligible actuator dynamics such as an electro-pneumatic or hydraulic actuator (see figure 1, lower part), is dithering. Dither is a high frequency signal with an amplitude greater than the maximum stick friction force, which is added to

the control signal to keep the system at a non-zero velocity and thus avoid stick-slip friction. However, this method is energy-consuming and some neglected dynamics may be excited.

3. Using a non-model-based observer for friction: A more recent non-model-based method [14] uses an adaptive friction force observer which can be either an extended Kalman-Bucy filter or a local function estimator. The observer output is used to compensate friction by adding a force or torque to the control signal with a value equal and -servo). opposite to instantaneous friction.

- Model-based approach: The other approach is model-based friction compensation. Its implementation requires choice of an appropriate friction model, identification of its parameters, and finally friction compensation using the identified model. This also assumes that force or torque actuation of adequate bandwidth is available and stiffly coupled to the friction element. Then, friction compensation is obtained by adding the opposite of the predicted friction to the control signal, as shown in figure 1. The main disadvantage of this approach is that friction compensation in a servo with an actuator of non negligible dynamics, such as pneumatic-servo (figure 1, lower part) is not as straightforward as in a dc-motor-driven system (figure 1, upper part). However, electro-pneumatic actuators use air that is clean and inexpensive. They can provide high power for large loads and, compared to the dc-motors, no heavy motors with complex gearing are required. To cope with the presence of actuator dynamics, one possibility is to use an inner force control loop, in addition to the position control loop, as shown in figure 2. This strategy has already been used for position control in hydraulic-actuator in the presence of friction [17] (the actuator dynamics of the hydraulic-servo is similar to that of the pneumatic-servo).

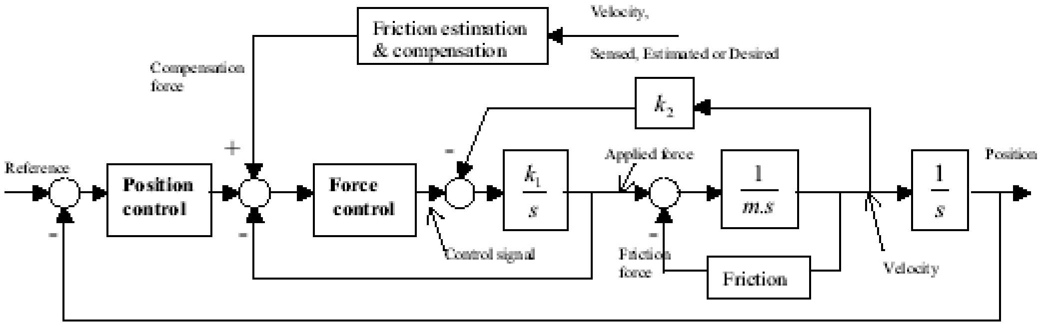

Figure 2: Force control, position control and model-based friction compensation in an electro-pneumatic actuator.

The diagram in figure 2, can be used to:

- eliminate the position steady-state error produced by friction, when the position controller is PD.
- eliminate the position oscillation produced by friction, when the position controller is PI(D).

In this paper, the diagram in figure 2 is used for Karnopp model-based friction compensation in an electro-pneumatic servo. The aim is to eliminate the position steady state error (or to improve the position regulation performance), using two control loops (position and force).

The choice of the Karnopp model of friction [7] is explained in the companion paper [13], in which, a three-step method is presented for identifying the model parameters (see also [11]). The simulation and the experimental results using the electro-pneumatic actuator confirm the efficiency of the proposed identification method

Model-based friction compensation using the Karnopp model, in an electric-motor system, has been already used [3, 6, 12]. This compensator gives satisfactory results when the objective is position tracking. Compensator inputs are velocity and applied force. It seems that this compensator is not able to eliminate the steady state error because it does not consider the position error.

The contribution of this paper is two-fold:

1. Friction compensation based on the Karnopp model applied on an electro-pneumatic servo, which is a more difficult problem than an electric-actuator servo. For this objective, the diagram in figure 2 is used, where finally RST and PI controllers are used for the two control loops (position and force, respectively), with fixed parameters during friction compensation procedure. The force loop controller is a simple PI controller. The parameters of the RST controller are found using pole placement method and an identified model of the system including the force loop. For other papers dealing with friction compensation and in which control performance is also considered based on system identification, see [5, 16, 9, 2, 17].

2. Improvement of the position steady state error or position limit cycle elimination using the value of the position error in the compensation structure for very low velocity values.

The paper is organized as follows: the asymmetrical Karnopp model is briefly reviewed in section 1. Section 2 describes the proposed model-based compensation method. In section 3, experiment design is explained and the results (simulation and real-time) obtained for the electro-pneumatic actuator are illustrated.

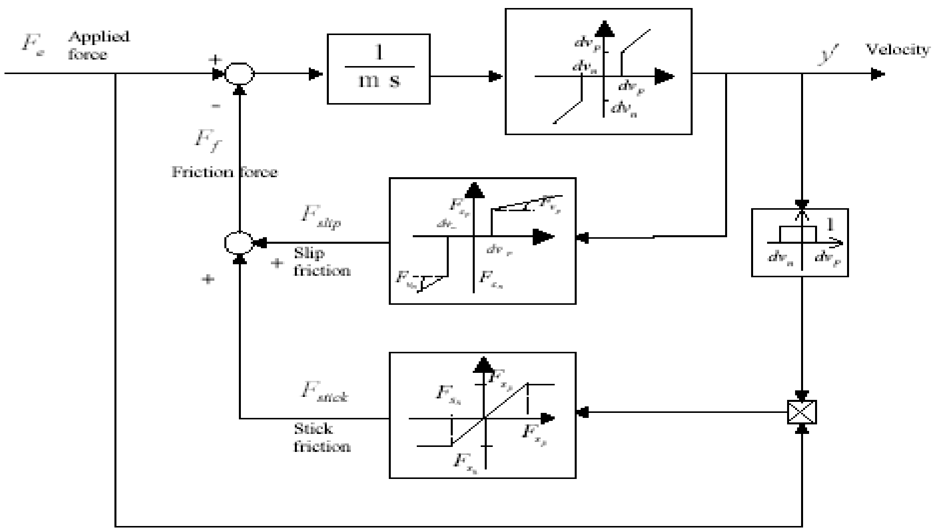

Figure 3: Block diagram of an asymmetrical Karnopp model.

1. ASYMMETRICAL KARNOPP MODEL

In this section, a brief presentation of the asymmetrical Karnopp model is given. For more information, readers can refer to the section 1 of the companion paper [13] or [11].
Figure 3 illustrates an asymmetrical Karnopp model. The nine model parameters are: m (mass of the moving part), F_{cp} ; F_{cn} (Coulomb friction for positive and negative velocity), F_{vp} ; F_{vn} (viscous friction coefficient for positive and negative velocity), d_{vp}; d_{vn} (limited velocity in stick-positive slip and stick- negative slip regions) and F_{sp} ; F_{sn} (maximum and minimum stick friction). Thus, the vector of the model parameters is

$$P_{asym} = [m,\ F_{c_p},\ F_{c_n},\ F_{v_p},\ F_{v_n},\ dv_p,\ dv_n,\ F_{s_p},\ F_{s_n}].$$

All the model parameters are positive, excepted for F_{sn} and d_{vn}.
The other symbols in the figure are: $\dot{y}\,(t)$ (velocity),$F_c(t)$ (applied external force) and $F_f\,(t)$ (friction force), which is characterized by:

$$F_f(t) = \begin{cases} F_{slip}(t) = \begin{cases} F_{c_p} sign(\dot{y}(t)) + F_{v_p}.\dot{y}(t) & \dot{y}(t) \geq dv_p \\ F_{c_n} sign(\dot{y}(t)) + F_{v_n}.\dot{y}(t) & \dot{y}(t) \leq dv_n \end{cases} \\ F_{stick}(t) = \begin{cases} min(F_e(t), F_{s_p}) & dv_n < \dot{y}(t) < dv_p, \quad F_e(t) \geq 0 \\ max(F_e(t), F_{s_n}) & dv_n < \dot{y}(t) < dv_p, \quad F_e(t) \leq 0 \end{cases} \end{cases} \quad (1)$$

2 FRICTION COMPENSATION USING AN ASYMMETRICAL KARNOPP MODEL

Based on the identified parameters $\hat{P}_{asym}$, using the method presented in [13] or [11], the first idea for friction compensation, in the structures shown in figures 1 and 2, may be:

$$F_{comp} = \hat{F}_f = F_f(\hat{P}_{asym}) \quad (2)$$

where F_f is given by (1). From (1) it can be seen that compensator inputs are velocity, $\dot{y}$, and applied force, F_e.

The main disadvantage of this compensator is that its output, $\hat{F}_f$, is zero if $\dot{y} = 0$ and $F_e = 0$, even if the position-error, $e_y = r - y$, is not zero. This means that position regulation cannot be perfectly performed, when PD controller for position is used. If a PID controller is used, or an RST controller with an integral action, then the steady-state error is eliminated, but limit-cycle are probably to appear.

To eliminate the steady state error, the friction compensator structure (1) must use the position error, c$_y$, when velocity is in a narrow boundary around zero value, *i.e*

$$\frac{dv_n}{N_c} \leq \dot{y} \leq \frac{dv_p}{N_c}, \quad N_c > 1.$$

For this objective, a small positive threshold value, e_T, is considered for the position error. The compensation force, when velocity is in the boundary, is computed according to e_y, e_T and the stick friction parameters, $\hat{F}_{sp}$, $\hat{F}_{sn}$, as follows:

- If the position-error is large
  $$(|e_y| \geq e_T),$$
  a strong compensation force is needed. In this case, the compensation force, $\hat{F}_f$, is either equal to maximum stick friction, $\hat{F}_{sp}$, if $e_y > 0$, or equal to minimum stick friction, $\hat{F}_{sn}$, if $e_y < 0$.
- If the position-error is not large
  $$(|e_y| < e_T),$$
  then the compensation force, $\hat{F}_f$, is proportional to the maximum or minimum stick friction (according to the sign of e_y), by a gain equal to the relative position error, $\frac{e_y}{e_T}$.

  Therefore, compensation force at very low velocities is:

$$\hat{F}_{\text{zero-velocity}} = \begin{cases} min(\frac{e_y}{e_T}\hat{F}_{s_p}, \hat{F}_{s_p}) & e_y \geq 0, \quad \frac{\hat{dv}_n}{N_c} \leq \dot{y} \leq \frac{\hat{dv}_p}{N_c} \\ max(-\frac{e_y}{e_T}\hat{F}_{s_n}, \hat{F}_{s_n}) & e_y \leq 0, \quad \frac{\hat{dv}_n}{N_c} \leq \dot{y} \leq \frac{\hat{dv}_p}{N_c} \end{cases} \quad (3)$$

The presence of viscous friction force $\hat{F}_{vp} \cdot \dot{y}(t)$ and $\hat{F}_{vn} \cdot \dot{y}(t)$ introduces noise directly in the compensator structure (1), because velocity, $\dot{y}(t)$ is computed numerically from the measured position.To avoid this problem, the viscous friction force will be ignored in the compensation structure, as in other model-based friction compensation approaches [1]. Finally, the compensation force, F_{comp}, which will be used in the following, is:

$$F_{comp} = \begin{cases} \hat{F}_{slip_p} = \left\{ \hat{F}_{c_p} \quad \dot{y} \geq \hat{dv}_p \right. \\ \hat{F}_{slip_n} = \left\{ -\hat{F}_{c_n} \quad \dot{y} \leq \hat{dv}_n \right. \\ \hat{F}_{stick} = \begin{cases} min(F_e(t), \hat{F}_{s_p}) & \dot{y} \in (\hat{dv}_n,\ \hat{dv}_{n1}] \cup [\hat{dv}_{p1},\ \hat{dv}_p), \quad F_e \geq 0 \\ max(F_e(t), \hat{F}_{s_n}) & \dot{y} \in (\hat{dv}_n,\ \hat{dv}_{n1}] \cup [\hat{dv}_{p1},\ \hat{dv}_p), \quad F_e \leq 0 \end{cases} \\ \hat{F}_{\mathbf{zero-velocity}} = \begin{cases} min(\frac{e_y}{e_T}\hat{F}_{s_p}, \hat{F}_{s_p}) & \hat{dv}_{n1} < \dot{y} < \hat{dv}_{p1}, \quad e_y \geq 0 \\ max(-\frac{e_y}{e_T}\hat{F}_{s_n}, \hat{F}_{s_n}) & \hat{dv}_{n1} < \dot{y} < \hat{dv}_{p1}, \quad e_y \leq 0 \end{cases} \end{cases} \tag{4}$$

where $\hat{dv}_{p1} = \frac{\hat{dv}_p}{N_c}$ and $\hat{dv}_{n1} = \frac{\hat{dv}_n}{N_c}$, $N_c > 1$.

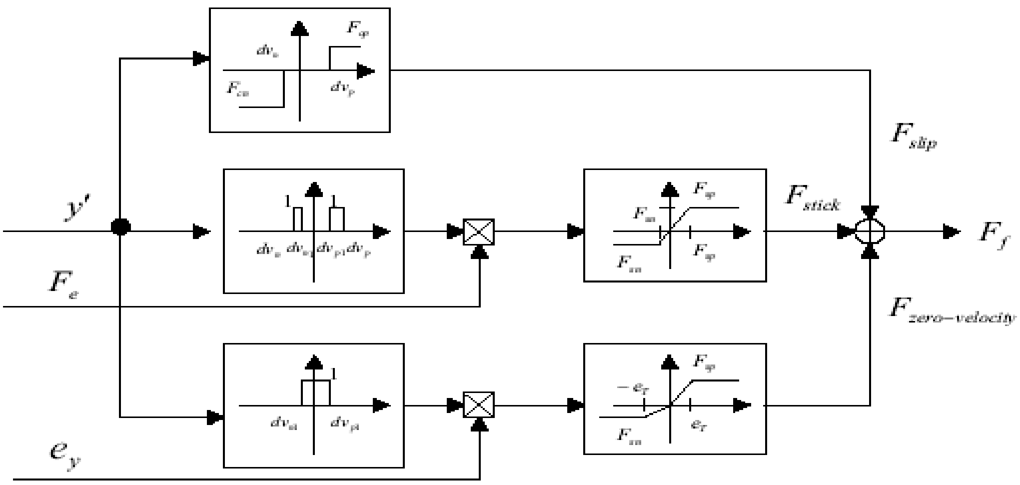

Figure 4: Friction compensation diagram using the Karnopp model.

Figure 4 shows the friction compensation block diagram using the Karnopp model and the zero-velocity compensation term. For notation simplicity, the ^ symbol is avoided.

As the $\hat{F}_{stick}$ component of this compensator acts on a very narrow band of velocity values, it can be sometimes ignored, the compensation performance is not very much affected. This can be seen from the application results. However, in order to be in the same line as the previous compensation techniques presented in the references cited in the introduction of the paper, the component $\hat{F}_{stick}$ is kept in the compensator structure. The effect of neglecting this component will be discussed in the application section.

Remark:

When choosing the compensator variables, *i.e* N_c and e_T , the following facts must be observed:

- The participation of compensation at zero-velocity in the compensation structure is more restricted for larger values of N_c, which results in the greater position steady-state error.
- The steady-state error is smaller for smaller values of e_T . However, the smaller e_T is, the more the compensator structure is sensitive to position error noise. This means that under the influence of noise, the compensation force switches from compensation at zero-velocity to compensation at stick periods (and vice versa). This switching produces oscillations in compensation force and in position.

3 APPLICATIONS

In this section, the experiment design, the simulation and the real time results for an electro-pneumatic actuator are presented, to show the improvement of position regulation performance when friction compensator (4) is used. The systems are the same as the ones in the companion paper [13].

In the simulation and real time experiments, the asymmetrical Karnopp models identified in the companion paper [13] or [11] are used.

3.1 Experiment design

In order to use the model-based friction compensation in figure 2, where F_{comp} is given in (4), the following facts have to be taken into account:

- The inputs of the "friction estimation and compensation" block are velocity, position-error and applied force, where the last two signals are also used in the position control loop and in the force control loop, respectively. These inputs are computed as follows:
  - Velocity is found by numerical derivation of the position. To limit the noise influence of the measured position y_m, a high order low pass filter must be used. This filter is called Filter *A*. Using the filtered position, y_f, the velocity , *i.e* $\dot{y}_f$, is computed as follows [8]:

$$\dot{y}_f(k) = \frac{1}{h}\frac{\sum_{i=1}^{N_d} i \ \sum_{i=1}^{N_d} y_f(k-i+1) - N_d \sum_{i=1}^{N_d} i.y_f(k-i+1)}{N_d \sum_{i=1}^{N_d} i^2 - (\sum_{i=1}^{N_d} i)^2} \qquad (5)$$

    where h is the sampling period. A time horizon Nd of 5 samples is used as in [8].
  - The position-error is the difference between the position reference and the position. Once more, to limit the noise influence, a filtered position signal can be used. This filter is called Filter *B*.
  - The applied force is measured in the simulation experiment (denoted by F_{ef}), and is computed in the real-time experiment (denoted by F_{ec}) from the pressure measurements. The realtime experience shows that the noise of the pressure measurements does not greatly influence compensation performance. Thus, no filter is used for the applied force.
- The output of the "friction estimation and compensation" block, F_{comp} may have very high frequency due to noise presence. Therefore, the computed compensation force F_{comp} is passed through a low pass filter (called Filter *C*) before being applied as compensation force F_{compf} . To improve the position error, this filter must allow a compensation force with sufficient amplitude and frequency to be applied. The experiments show that, to eliminate steady-state error, there is no need for a high frequency compensation force. Thus, a small cut-off frequency value of this filter is considered. This choice also has the advantage of decreasing noise influences.
- The controllers and the friction compensator use the signal values expressed in their physical units. For this reason, all measured signals are multiplied by the inverse of their sensor gains.

3.2 Simulation results

The block diagram in figure 5 presents a linear model of an electro-pneumatic actuator with model-based friction compensation using the Karnopp model.

The block diagram is simulated using the true Karnopp model parameters (for the system) and the estimated Karnopp model parameters [13] (for the friction estimator). These values are given in table 1. The actuator parameters are $k_1 = 19530\ V^{-1}.\ N.sec^{-1}$ and $k2 = 10405\ N.m^{-1}$. The sampling period $h = 10^{-3}\ s$ is used. The gain of position sensor is $g_y = 1\ m^{-1}V$ and the gain of force sensor is $g_F = 1\ N^{-1}V$. The measurement noises n_{Fe} , n_y, are Gaussian signals with zero mean and of variances 10^{-4} and 10^{-10}, respectively.

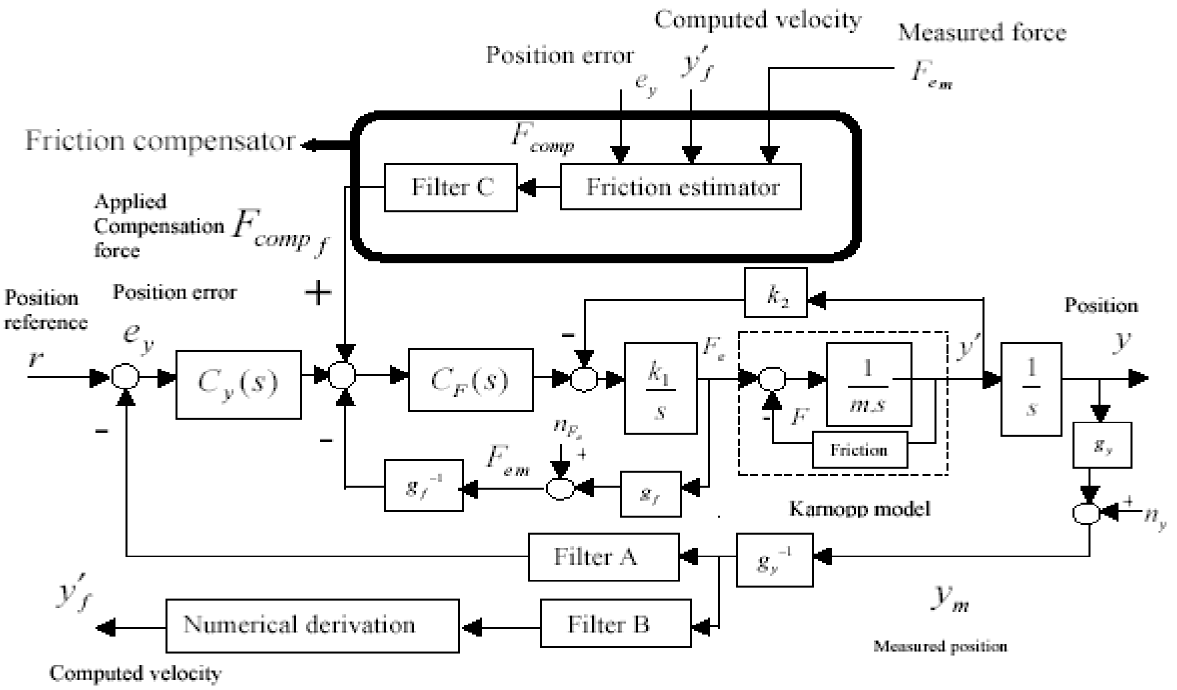

Figure 5: Block diagram used to test the proposed model-based friction compensation in simulation.

	$[N]$		$[N\frac{m}{s}]$		$[kg]$	$[\frac{m}{s}]$		$[N]$	
Parameter	F_{c_p}	F_{c_n}	F_{v_p}	F_{v_n}	m	dv_p	dv_n	F_{s_p}	F_{s_n}
True value	12	15	300	200	1	0.04	−0.04	20.6	−23
Estimated value	13.4	13	264.8	210.3	0.85	0.026	−0.041	22.8	−25.2
Standard deviation	1.74	2.56	20.35	26	0.028	0.0025	0.001	1.03	0.74
Error	12%	13.6%	11.7%	5.2%	14.8%	35.5%	1.7%	10.8%	9.7%

Table 1: True and estimated values of the Karnopp model parameters.

The low-pass filters *A*, *B* and *C*, are all 40 order FIR filters with cut-off frequency 5 *Hz*.

The force controller, C_F , and the position controller, C_y, are:

$$C_F(s) = k_i(1+\frac{1}{T_i s}) \text{ and } C_y(s) = k_d(1+\frac{T_d s}{\epsilon s+1})$$

where $ki = 0.02\ V\ N^{-1}$, $Ti = 0.05\ s$, $k_d = 200$, $T_d = 0.1\ s$ and $\epsilon = 0.2\ s$.

In the compensator structure (see equation (4)), $N_c = 2$ and $e_T = 3\ mm$. The simulation results are shown in figures 6 and 7.

In figure 6, the influence of compensation at zero velocity is also shown. As can be seen, the steady state error due to the presence of friction cannot be completely eliminated if the compensation at zero velocity is not used.

In figure 7, the applied compensation force et computed velocity are shown.

In order to test the effect of an integral action in the position control, a PID controller has been used instead of the previous PD controller. The PID controller has the following structure:

(6) $$C_y(s) = k_R(1+\frac{1}{T_i s}+\frac{T_d s}{\epsilon s+1})$$

where the coefficients are: $k_R = 1754$, $T_d = 0.018\ s$, $T_i = 0.072\ s$, and $\epsilon = 0.2\ s$.

The steady-state error is eliminated, but position limit-cycle appear (see fig. 8). These limit-cycles can be lowered if a more complex position controller is used, as it will be shown in the next section.

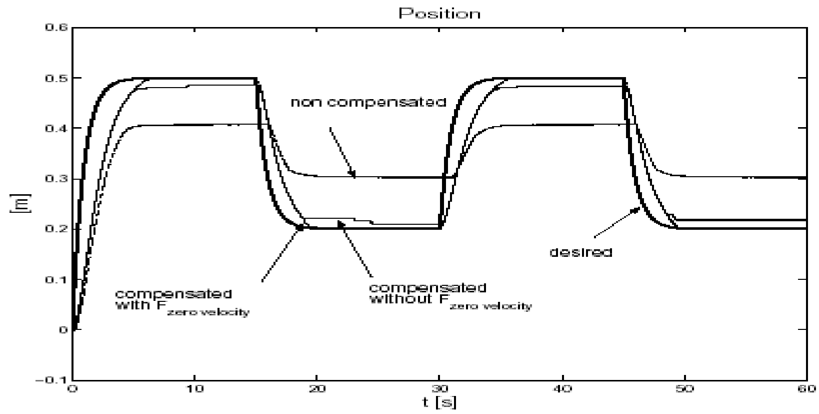

Figure 6: Desired position (thick line), position with compensation (two thin lines) and without compensation. (dashed line), in simulation.

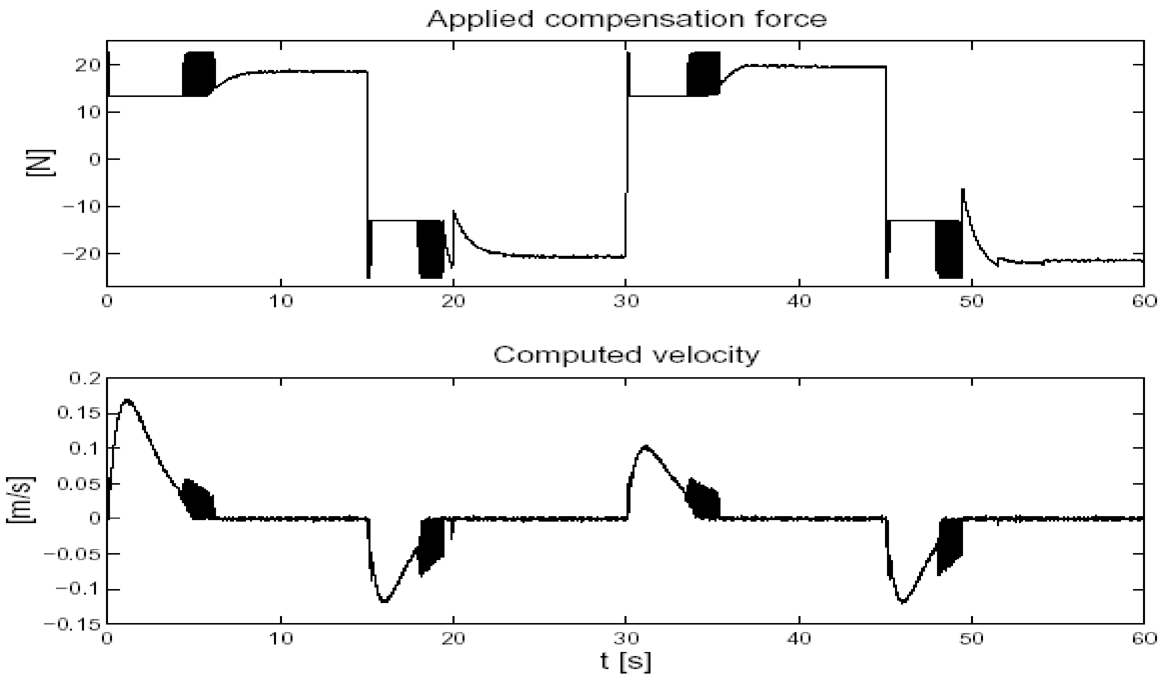

Figure 7: Applied compensation force, *Fcompf* , and computed velocity, $\dot{y}_f$, in simulation.

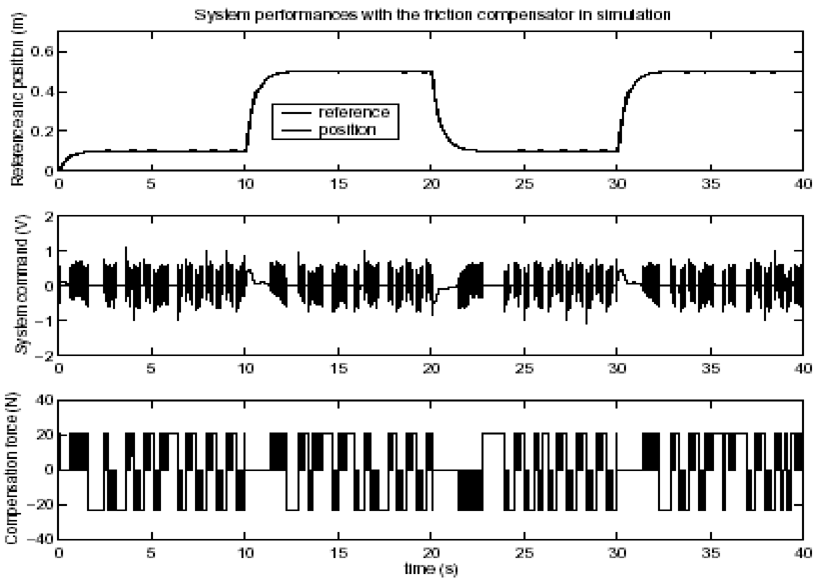

Figure 8: Desired (reference) and obtained position, with compensation and PID position control, in simulation. Associated control signal (command) and applied compensation force

3.3 Real-time experiment

The real-time experiment consists of an electro-pneumatic actuator with friction phenomena.

An important point with friction phenomena and with mechanical systems is that system can change with time and the control performances can worsen. It is shown in this example that friction parameters have to be re-identified and compensator parameters updated after a period of time, in order to cope with system changes.

In order to find the optimal configuration of the ensemble compensator and control loops for good position tracking, different control configurations for the position loop have been tested. The force loop is always realized with a PI controller, while for the position loop several controllers has been tested, with increasing order of complexity as follows: PD, PID and RST controller.

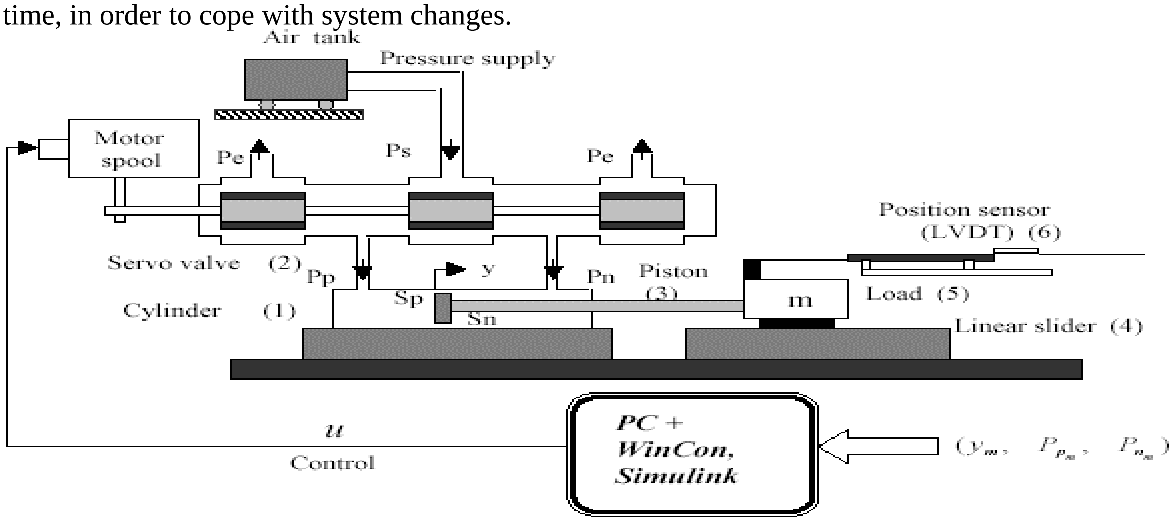

Figure 9: Experimental test apparatus.

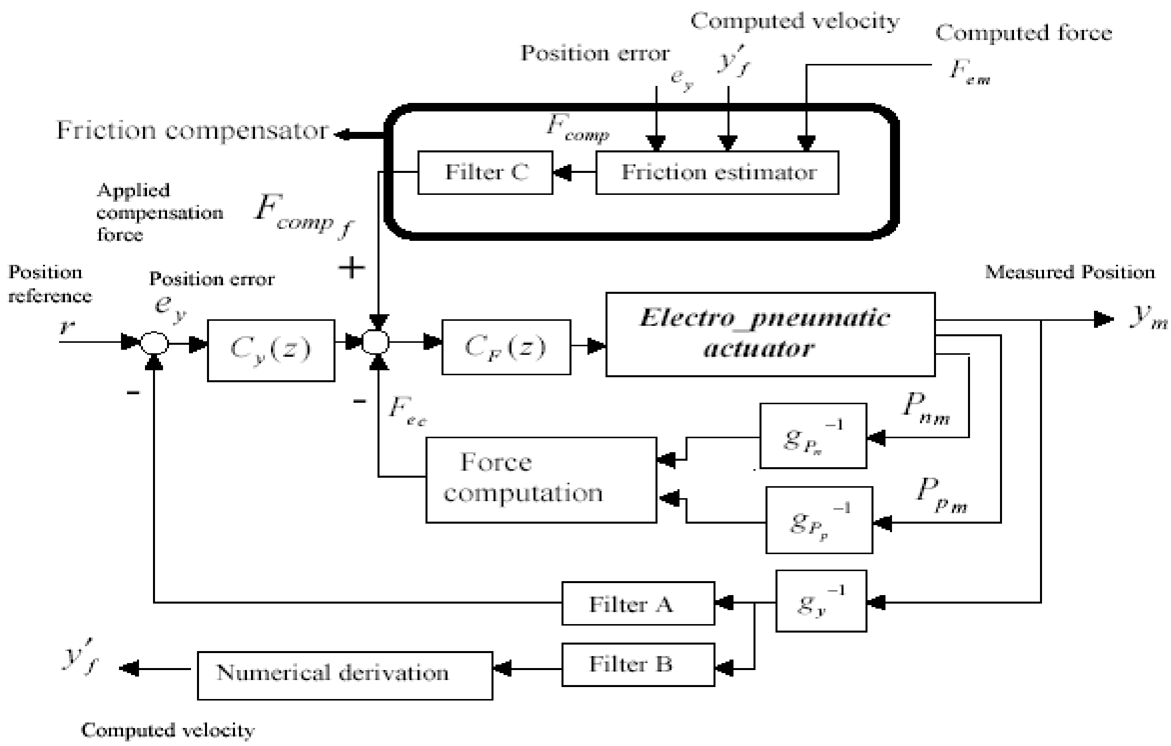

Figure 10: Set-up used for model-based friction compensation (real-time experiment).

3.3.1 Physical system

The physical system, shown in figure 9, consists of an electro-pneumatic cylinder (1) controlled by an electro-pneumatic and proportional servo-valve (2). The cylinder piston (3) is attached to a linear slider (4) carrying a load (5) on which friction force, a net force proportional to the pressure difference in cylinder and external disturbances, acts. The position $y(t)$ is measured using a Linear Variable Differential Transducer (6), while the control signal $u(t)$ is the servo-valve input current. The hardware and software connection is performed by Win Con and Simulink programs. During the experiment, the sampling period is equal to $h = 0.01\ s$.

3.3.2 Model-based friction compensation

The set-up presented in figure 10 is used. The estimated Karnopp model parameters [13] (used in the friction estimator) are given in table 3.
The measured signals are the pressure in the right and left chambers of the cylinder, P_{pm} and P_{nm}, and the position, y_m. The position sensor gain is $g_y = 80\ V\ m^{-1}$ and the pressures sensor gains are equal to $gP_p = gP_n = 10^{-5} V\ Pascal^{-1}$.
In the experimental electro-pneumatic actuator, the applied force $Fe(t)$ cannot be measured and can be computed as

$$F_{e_c}(t) = S_p.P_{p_f} - S_n.P_{n_f} - (S_p - S_n).P_s \quad (7)$$

where F_{ec} is the computed applied force, P_{pf} and P_{nf} represent the filtered measured pressures and P_s is the supply pressure. S_p and S_n are respectively the area of the right and left chambers of the cylinder. For the experimental system these areas are $S_p = 12.6\ cm^2$ and $S_n = 10\ cm^2$. The low-pass filters A and C are chosen as

$$\frac{0.5}{1-0.5z^{-1}} \text{ and } \frac{0.2}{1-0.8z^{-1}}.$$

Filter B is a 40 order FIR filter with cut-off frequency 10 Hz. This filter introduces a delay of $(40/2+1)h = 0.21\ s$ between the measured position and the estimated velocity. However, the experiment shows that it does not influence position regulation performance.

The force controller, C_F , and the position controller, C_y, are sampled-time versions of PI and PD controllers respectively:

$$C_f(z) = k_i\left(1+\frac{hz^{-1}}{T_i(1-z^{-1})}\right) \text{ and } C_y(z) = k_d\left(1+\frac{T_d(1-z^{-1})}{\epsilon(1-e^{\frac{-h}{\epsilon}}z^{-1})}\right)$$

where $ki = 0.03\ V\ N^{-1}$, $Ti = 0.75\ ms$, $k_d = 500\ Nm^{-1}$, $T_d = 0.02\ s$, $\epsilon = 0.2\ s$ and $h = 0.01\ s$.

In the compensator structure (see equation 4), $N_c = 2$ and $e_T = 5\ mm$. As figure 11 illustrates, the steady state error due to the presence of friction is completely eliminated using the Karnopp-based friction compensator (4).

In the same figure, the control signal (u in figures 9 and 10) is shown for the two cases, without and with compensation. The control signal is more active in the case with compensation.

Figure 12 shows the applied compensation force, F_{compf} , and the computed compensation force, F_{comp}. Friction compensation at the positive, negative, stick and zero velocity periods is illustrated in figure 13. In the same figure, computed velocity is also shown.

	$[N]$		$[N\frac{m}{s}]$		$[kg]$	$[\frac{m}{s}]$		$[N]$	
	$\hat{F}_{c_p}$	$\hat{F}_{c_n}$	$\hat{F}_{v_p}$	$\hat{F}_{v_n}$	$\hat{m}$	$\hat{dv}_p$	$\hat{dv}_n$	$\hat{F}_{s_p}$	$\hat{F}_{s_n}$
Value	16.97	18.13	289	287.4	3.5	0.009	-0.01	20.76	-21.8

Table 2: Estimated values of the asymmetrical Karnopp model parameters for the electro-pneumatic actuator.

3.3.3 Sensitivity to system parameters

The experimental tests have been repeated after a long time period, using the same compensator and controller parameters. The obtained results are shown in fig. 14, where important differences can be observed compared with the previous ones.

If a PID controller is used for the position loop instead of a PD controller, the performances are not improved (see fig. 15). The PID coeficients have been obtained using pole placement method and an identified model of the system containing the force loop (the model nulerator is $B(z^{-1}) = -0.0012z^{-1}+0.004z^{-2}$; and the denominator is $A(z^{-1}) = 1\text{-}0.0604z^{-1}\text{-}0.9377z^{-2}$).

The obtained discrete time PID position controller is:

$$C_y(z) = \frac{176.7 - 335.7z^{-1} + 159.4z^{-2}}{1 - 1.68z^{-1} + 0.6799z^{-2}} \quad (8)$$

The force controller has been left unmodified:

$$C_F(z) = k_i\left(1 + \frac{hz^{-1}}{T_i(1 - z^{-1})}\right) \quad (9)$$

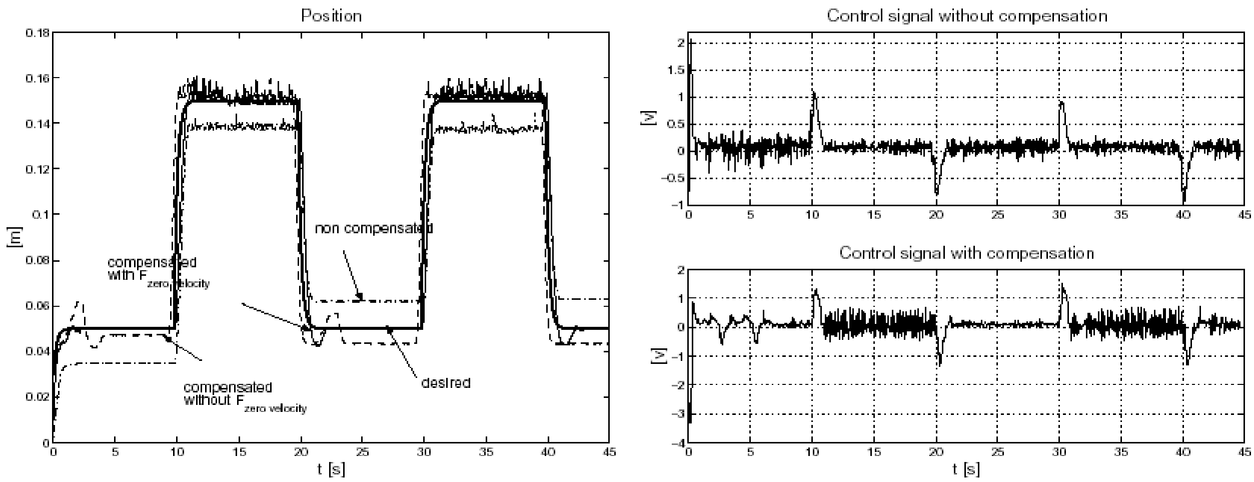

Figure 11: Left: desired position (thick line), position without compensation (dash-dot line), with $F_{\text{zero-velocity}}$ compensation (thin line) and without $F_{\text{zero-velocity}}$ compensation (dash line). Right: control signal with and without compensation, in real-time experiment.

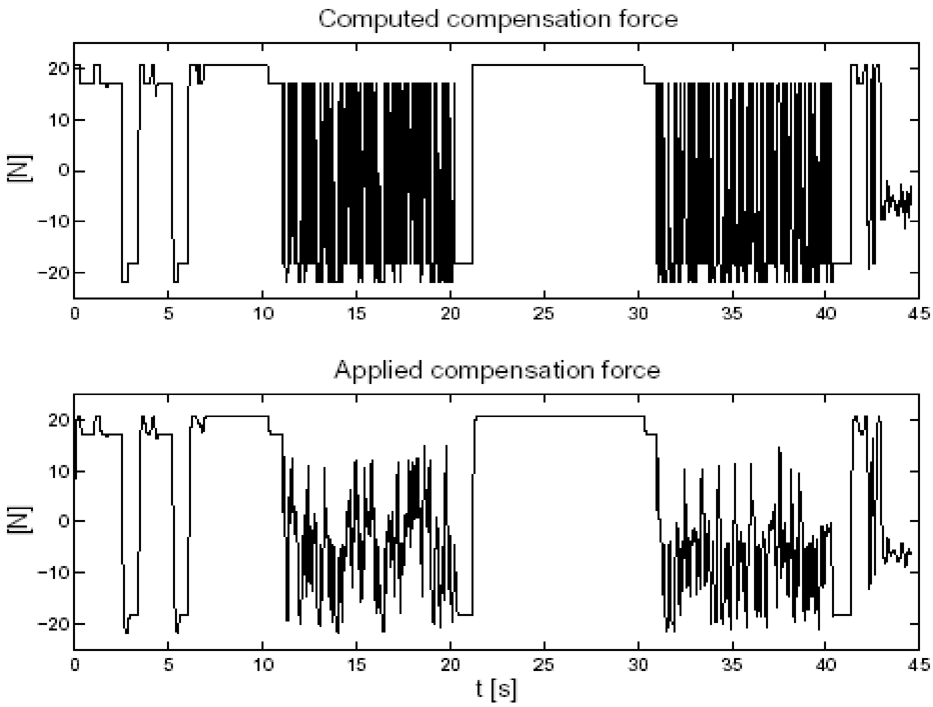

Figure 12: Computed and applied compensation force, in real-time experiment.

	$[N]$		$[N\frac{m}{s}]$		$[kg]$	$[\frac{m}{s}]$		$[N]$	
	$\hat{F}_{c_p}$	$\hat{F}_{c_n}$	$\hat{F}_{v_p}$	$\hat{F}_{v_n}$	$\hat{m}$	$\hat{dv}_p$	$\hat{dv}_n$	$\hat{F}_{s_p}$	$\hat{F}_{s_n}$
Value	12.54	7.35	147.01	113.05	6.5	0.015	−0.02	24.03	−10.18

Table 3: Estimated values of the asymmetrical Karnopp model parameters for the electro-pneumatic actuator.

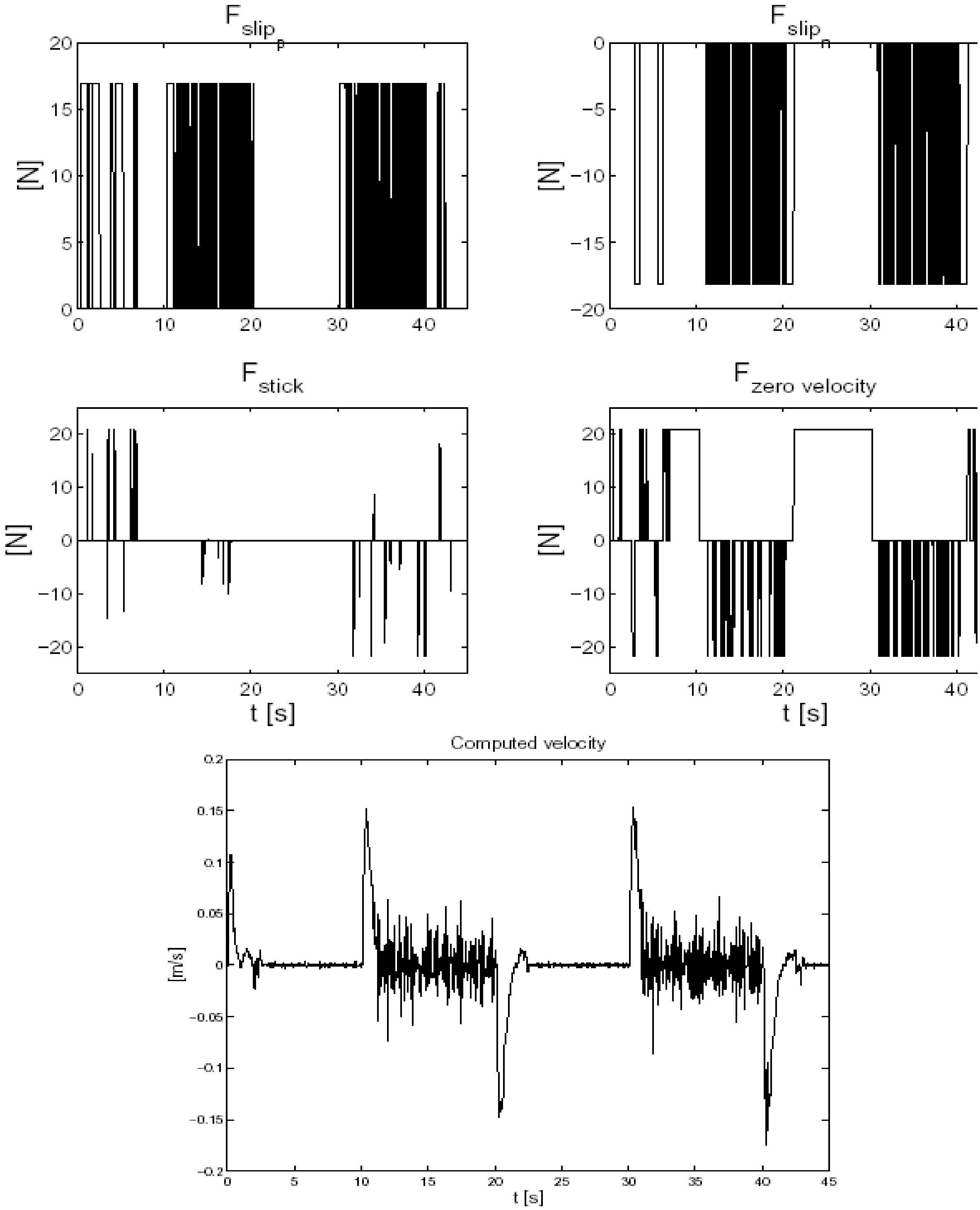

Figure 13: Estimated frictions in equation (4) and computed velocity, in real-time experiment.

3.3.4 Friction parameters up-date and position control-loop optimization

Friction parameters have been up-dated from a new identification experiment using the method presented in [13], and their new values are given in table 3.

Firstly, a PID position controller has been used. Figure 16 shows the system performances including the applied command to the system and the applied compensation force friction compensator with the newly identified parameters is used

Figure 17 presents the calculated components of the Karnopp model based friction compensator. In figure 21 the computed velocity is shown. In order to optimize the position tracking, a more complex position controller than the PI has been designed.

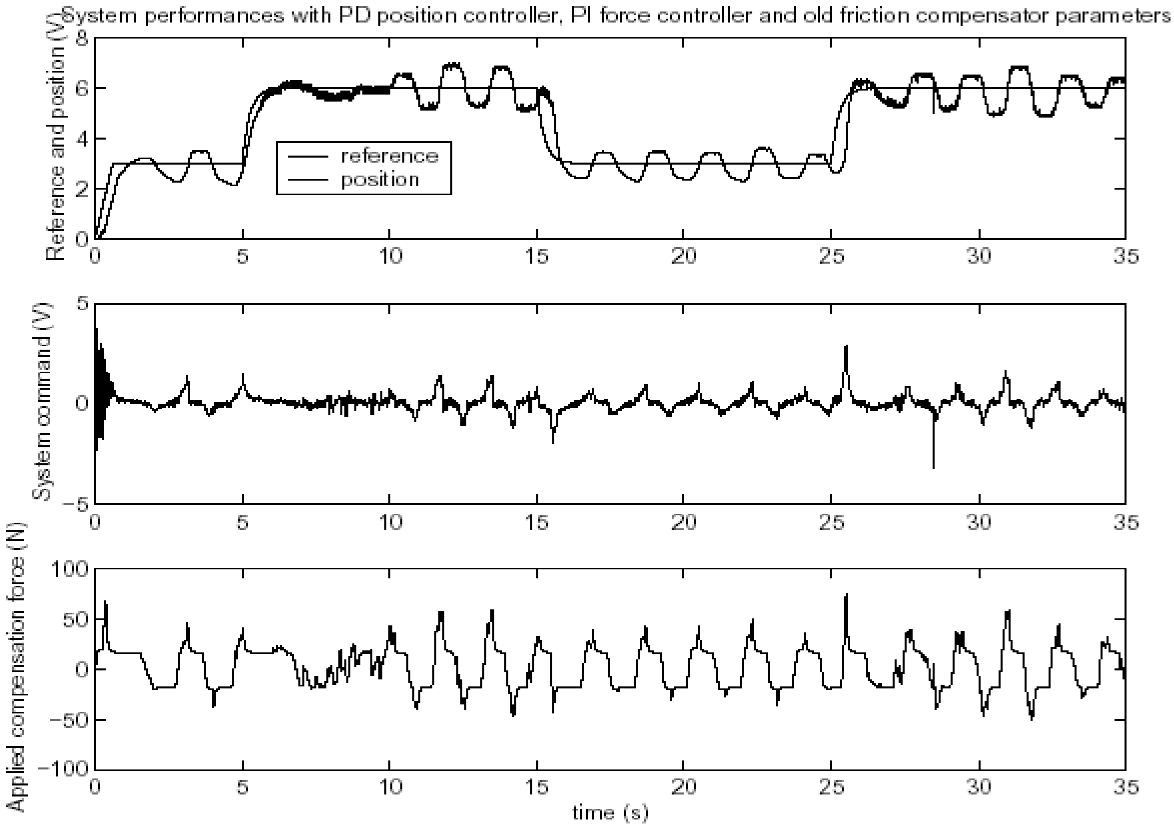

Figure 14: System performances using PD position controller and PI force controller with original friction compensator parameters.

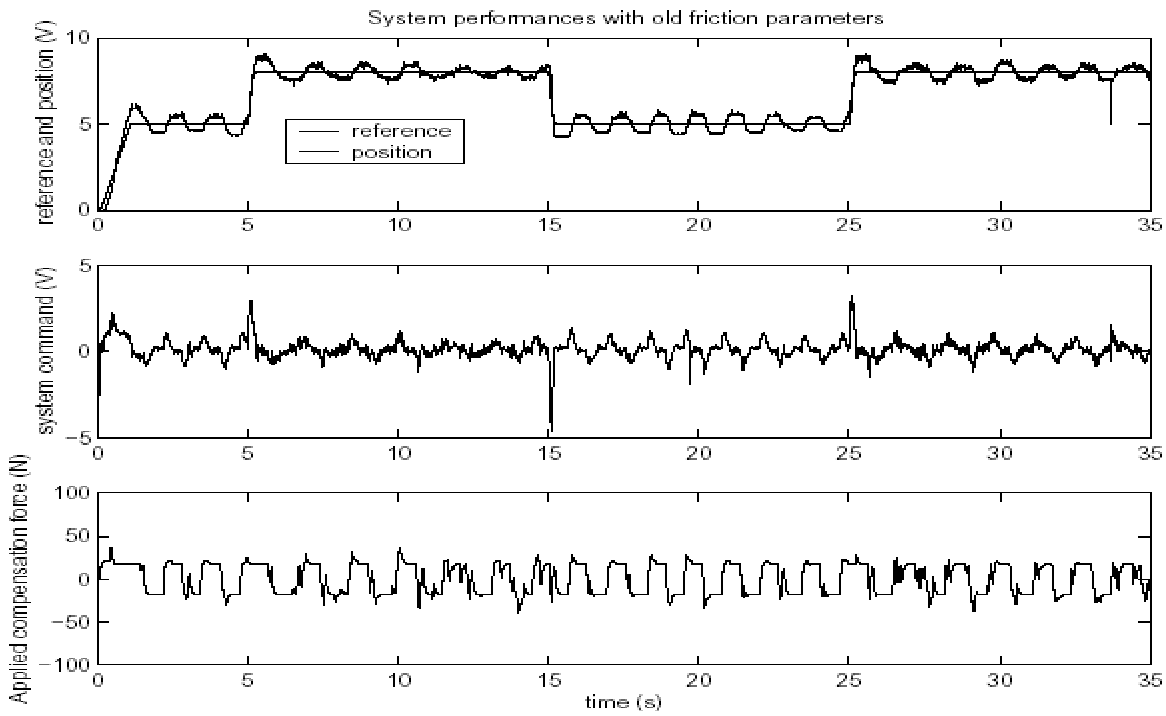

Figure 15: System performances using PID position controller and PI force controller with original friction compensator parameters.

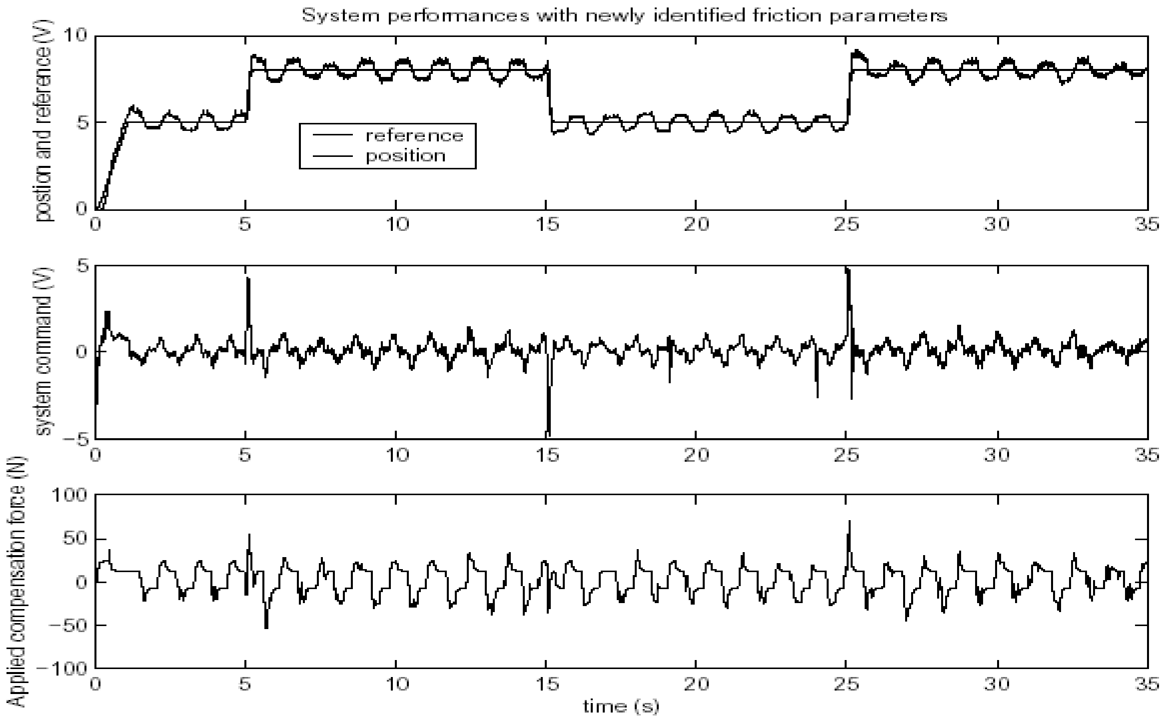

Figure 16: System performances using PID position controller and PI force controller with new friction compensator parameters.

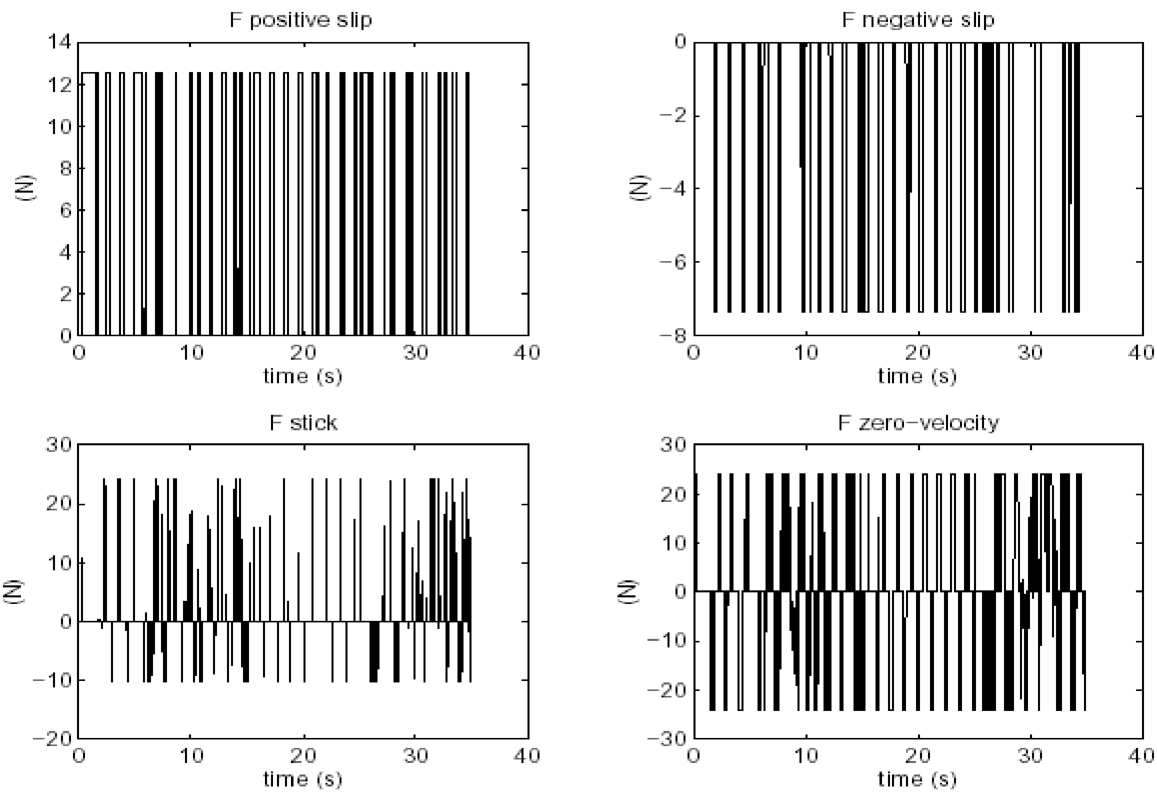

Figure 17: Estimated friction components of the compensator.

The structure of this controller is RST (with three polynomials *R; S; T*), see [10]. The following model for the system:

$B(z^{-1}) = 0.0001782z^{-3} + 0.0001322^{-4};$

$A(z^{-1}) = 1 - 2.142z^{-1} + 1.688z^{-2} - 0.5459z^{-3};$

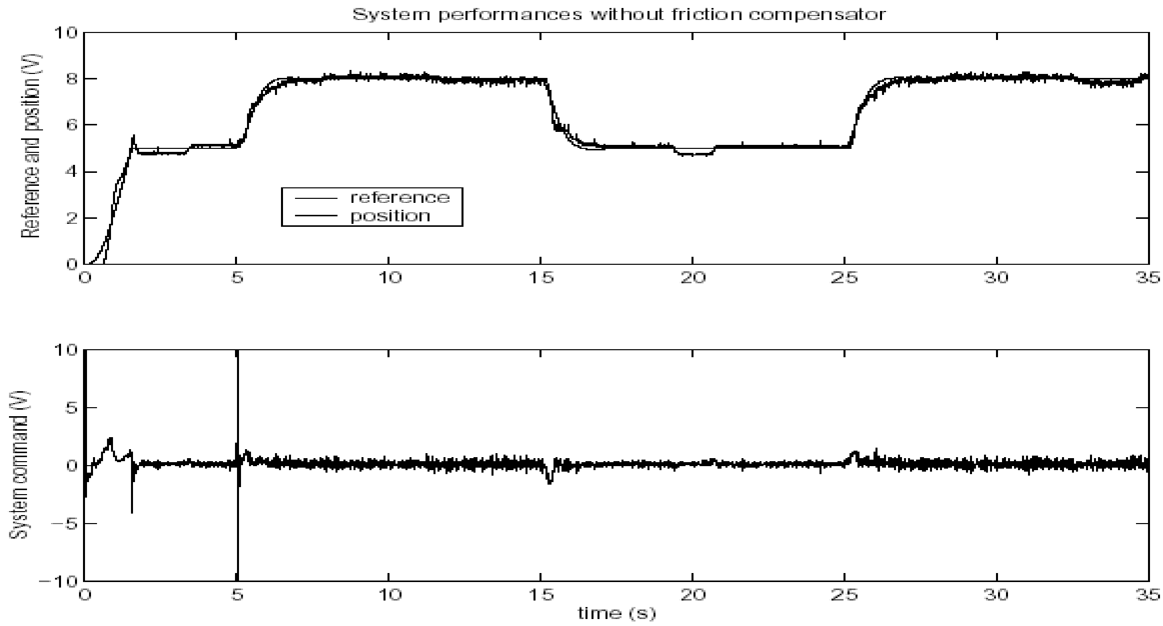

Figure 18: System performances using RST position controller and PI force controller without friction Compensator

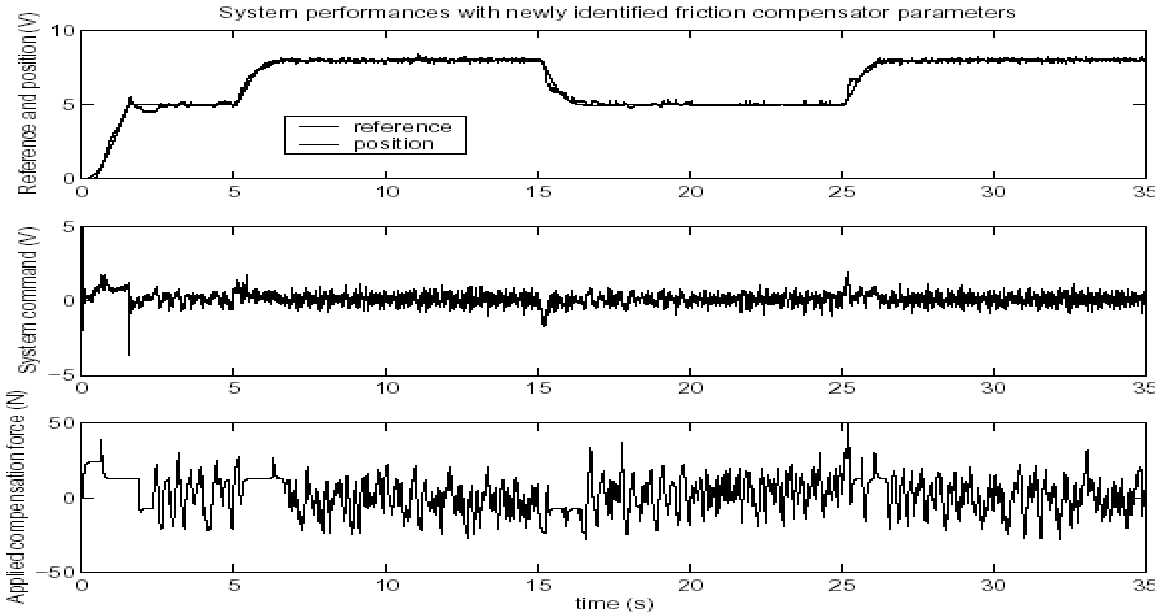

Figure 19: System performances using RST position controller and PI force controller with new friction compensator parameters.

The obtained RST coefficients are :

R = [-54.8202 172.7025 – 12.7034 – 102.5599 29.0003 – 28.0993 51.2437 – 75.9708 – 35.0083 59.046]

S = [1.0000 0.1901 – 0.3279 – 0.4677 – 0.3682 – 0.1987 – 0.0395 0.0583 0.0842 0.0550 0.0143]

T = 1000 * [3.2218 – 6.2898 3.0708]

This controller offers a good compromise between stability and complexity as a higher order controller can be less sensitive to noisy signals but needs a higher computation effort and a lower order controller is more sensitive to the noises present in the measured data. In the control structure the force controller remained the same.

The system performances without friction compensator are presented in figure 18. The squared error of the position tracking for the period between 5 *s* and 35 *s* is 70.641 $(i.e.\ \sum_{t=5\,s}^{35\,s}(ref(t)-y(t))^2)$. If the friction compensator with the new parameters is used the output error reaches 58.111, which shows the effect of friction compensation. See also fig. 19.

If the previous friction compensator coeffcients are used, the squared error is 72.029, which again demonstrates the sensitivity to the parameter changes over time periods.

Figure 20 shows the calculated components of the Karnopp model based friction compensator. In figure 21 the computed velocity is shown.

If from the friction compensator structure the F_{stick} component is removed, the obtained results are not much different than previously (see fig. 22).This means that this component is not determinant for the compensation performances. However, in this paper it has been kept as in other related papers cited in the reference. The performances of the system are presented in figure 22.

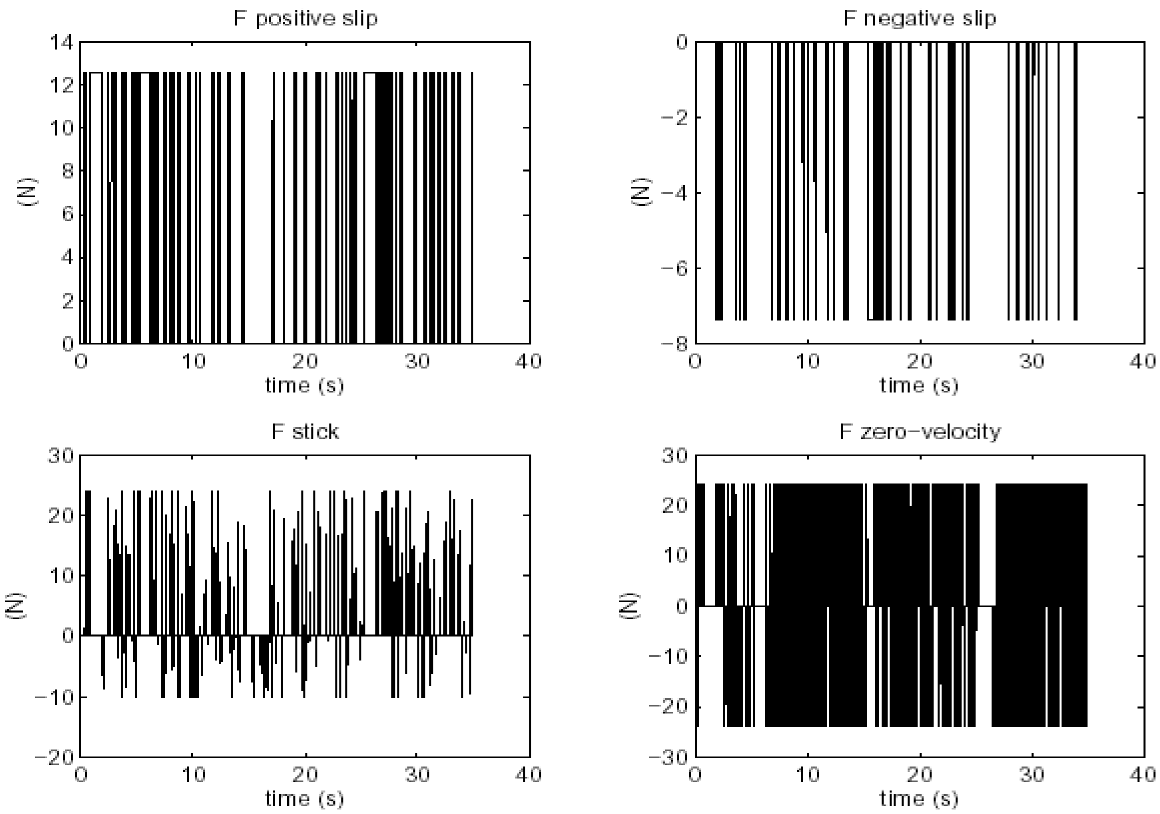

Figure 20: Estimated frictions of the friction compensator

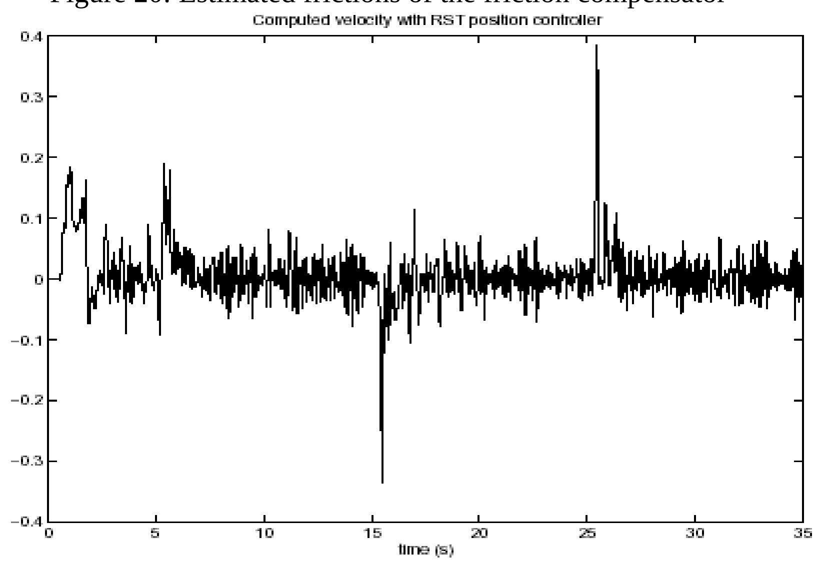

Figure 21: Computed velocity in the presence of the friction compensator.

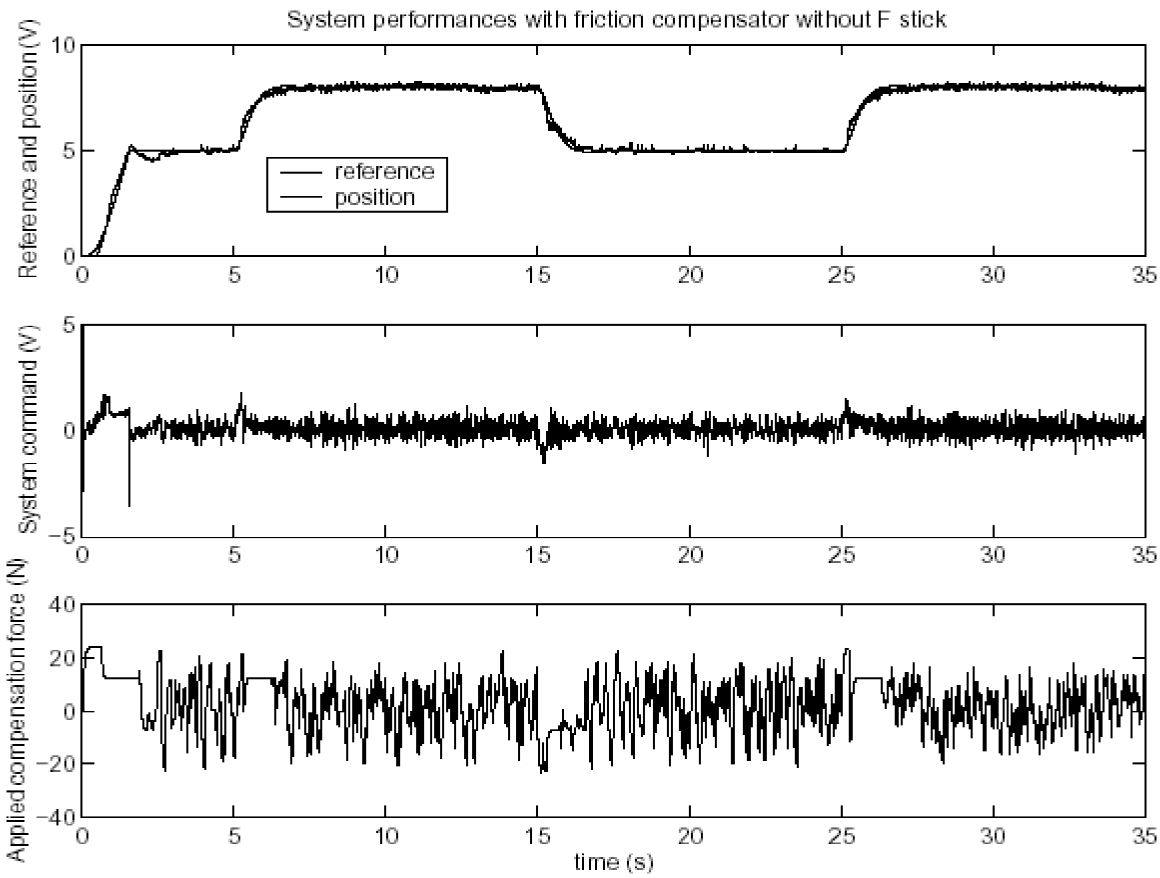

Figure 22: System performances using RST position controller and PI force controller with new friction compensator parameters without F_{stick}

4 CONCLUSION

In this paper model-based friction compensation using the asymmetrical Karnopp model for an electro- pneumatic-actuator has been presented. The complete control scheme consists of two loops (a position loop and a force loop) together with the friction compensator.

The main advantage of this control structure with friction compensation is that it realizes a good compromise between a relative simplicity and position tracking performances, despite disturbances and hard nonlinearities like measurement noise and friction.

The main characteristics of the friction compensator consists of considering the position error for near- zero velocities in the compensator structure.

However, a good position controller is very important for high performance reference tracking, and in this case a polynomial RST controller is superior to the PID controller for the position loop.

Implementation of the proposed friction compensator and control loops, on simulation and on an experimental electro-pneumatic servo, shows its efficiency in improving the position tracking.

5 ACKNOWLEDGEMENTS

The authors would like to thank Janosz Laszlo Ferenc (from Technical University of Iasi, Romania) for valuable experimental work realized in 2003 during his training period in Automatic Control Laboratory of Grenoble, allowing thus the comparisons between previous compensator parameters and new ones.

6. REFERENCES

[1] B. Armstrong-Hélouvry, P. Dupont, and C. Canudas de Wit. A survey of models, analysis tools and compensation methods for the control of machines and friction. *Automatica*, 30(7):1083{1138, 1994.

[2] J. E. Bobrow and K. Lum. Adaptive, high bandwidth control of a hydraulic actuator. *Proc. 1995 Amer Contr. Conf.*, pages 71{75, 1995.

[3] G. Brandenburg and U. Schäfer. Inffluence and compensation of coulomb friction in industrial pointing and tracking systems. *Proc. of the Industrial Application Society.*, pages 1407{1413, 1991.

[4] K. Hamiti, A. Besançon-Voda, and H. Roux-Buisson. Position control of a electro-pneumatic actuator under the influence of stiction. *Control Eng. Practice*, 4(8):1079{1088, 1996.

[5] C. H. Huang and Y. T. Wang. Self-optimization adaptive velocity control of asymmetric hudraulic actuator. *Int. J. Adaptive Contr. Signal Procesing*, 9(3):271{283, 1995.

[6] C. T. Johnson and R. D. Lorenz. Experimental identification of friction and its compensation in precise, position controlled mechanisms. *Proc. of the indus. App. Soc. Annual meeting*, pages 1400{ 1406, 1991. Dearborn, Michigan.

[7] D. Karnopp. Computer simulation of stick-slip friction in mechanical dynamic systems. *Journal Dynamic System Measurement Control*, 107(1):100{103, 1985.

[8] H. Keller and R. Isermann. Model-based nonlinear adaptive control of a pneumatic actuator. *Control Engineering Practice*, 1(3):505{511, 1993.

[9] A. Kotzev, D. B. Cherchas, and P. D. Lawrench. Performance of generalized predictive conttrol with on-line model order determination for a hydraulic robotic manipulator. *Robotics*, 13:55{64, 1994.

[10] I. D. Landau. *Identification et commande des systèmes*. Hèrmes Science Publications, Paris, 2nd edition, 1993. 34

[11] L. Ravanbod-Shirazi and A. Besançon-Voda. Identiffication of karnopp model parameters, a two step approach approach. *Proc. of of IEE conference on Control*, 2000.

[12] L. Ravanbod-Shirazi and A. Besançon-Voda. Robust friction compensation based on karnopp model. *Proc. of European Control conference*, pages 2558{2563, 2001.

[13] L. Ravanbod-Shirazi and A. Besançon-Voda. Friction identification using the Karnopp model, applied to an electro-pneumatic actuator. *Journal of Systems and Control Engineering, Proc. Instn Mech. Engrs*, 217:123{138, 2003.

[14] L. R. Ray, A. Ramasubramanian, and J. Townsend. Adaptive friction compensation using extednded kalman-bucy filter friction estimation. *Control Engineering Practice*, (9):169{179, 2001.

[15] C. N. Shen and H. Wang. Nonlinear compensation of a second and third order system with dry friction. *IEEE Trans. on Applications and Industry*, 83(71):128{136, 1990.

[16] M. C. Shih and Y. R. Sheu. The adaptive position control of an electro hydraulic servo cylinder. *JSME Int. J.*, 34(3):370{376, 1991.

[17] G. A. Sohl and J. E. Bobrow. Experiments and simulation on the nonlinear control of a hydraulic servosystem. *IEEE Trans. on Control sys. technology*, 7(2):238{247, 1999.

[18] E. D. Tung, Y. Urushisaki, and M. Tomizuka. Velocity friction compensation for machine tool feed drives. *Proc. 1993 American Control Conf.*, pages 1932{1936, 1993.